Segall, J. E., S. M. Block, and H. C. Berg. 1986. Temporal comparisons in bacterial chemotaxis. *Proc. Natl. Acad. Sci. USA* 83:8987–8991.

Shimizu, T. S., N. Le Novère, M. D. Levin, A. J. Beavil, B. J. Sutton, and D. Bray. 2000. Molecular model of a lattice of signalling proteins involved in bacterial chemotaxis. *Nature Cell Biol.* 2:1–5.

Sourjik, V., and H. C. Berg. 2000. Localization of components of the chemotaxis machinery of *Escherichia coli* using fluorescent protein fusions. *Mol. Microbiol.* 37:740–751.

Sourjik, V., and H. C. Berg. 2002a. Receptor sensitivity in bacterial chemotaxis. *Proc. Natl. Acad. Sci. USA* 99:123–127.

Sourjik, V., and H. C. Berg. 2002b. Binding of the *Escherichia coli* response regulator CheY to its target measured in vivo by fluorescence resonance energy transfer. *Proc. Natl. Acad. Sci. USA* 99:12669–12674.

12
Rotary Motor

The structure of the rotary motor was described in Chapter 9 (Fig. 9.3) and its assembly was discussed in Chapter 10. Here, I will say more about function. Given that the diameter of the motor is less than one-tenth the wavelength of light and that it contains more than 20 of different kinds of parts (Appendix, Table A.3), it is a nanotechnologist's dream (or nightmare).

Power Source

Flagellar motors of *E. coli* are not powered by adenosine triphosphate (ATP) the fuel that energizes muscles (Larsen et al., 1974), but rather by protons moving down an electrochemical gradient; other cations and anions have been ruled out (Ravid and Eisenbach, 1984). The work per unit charge that a proton can do in crossing the cytoplasmic membrane is called the protonmotive force, Δp. In general, it comprises two terms, one due to the transmembrane electrical potential difference, $\Delta\psi$, and the other to the transmembrane pH difference $(-2.3kT/e)\ \Delta pH$, where k is Boltzmann's constant, T the absolute temperature, and e the proton charge. At 24°C, $2.3kT/e = 59\,\text{mV}$. By convention, $\Delta\psi$ is the internal potential less the external potential, and ΔpH is the internal pH less the external pH. *E. coli* maintains its internal pH in the range 7.6 to 7.8. For cells grown at pH 7, $\Delta p \approx -170\,\text{mV}$, $\Delta\psi \approx -120\,\text{mV}$, and $-59\ \Delta pH \approx -50\,\text{mV}$. For cells grown at pH 7.7, $\Delta p \approx \Delta\psi \approx -140\,\text{mV}$. For a general discussion of chemiosmotic energy coupling, see Harold and Maloney (1996).

The dependence of speed on voltage has been measured in *E. coli* by wiring motors to an external voltage source. Filamentous cells were drawn roughly halfway into micropipettes, and the cytoplasmic membrane of the segment of the cell inside the pipette was made permeable to ions by exposure to the ionophore gram-

icidin S. An inert marker was attached to a flagellar motor on the segment of the cell outside the pipette, and its motion was recorded on videotape. Application of an electrical potential between the external medium and the inside of the pipette (the latter negative) caused the marker to spin (Fung and Berg, 1995). The rotation speed was directly proportional to Δp over the full physiological range (up to −150 mV). These experiments were done with large markers (heavy loads) at speeds less than 10 Hz. They have been repeated in a different way with small markers (light loads) at speeds up to nearly 300 Hz, and the rotation speed still appears proportional to Δp (Gabel and Berg, 2003).

The only measurement of proton flux that has been made is with motors of the motile *Streptococcus* sp. strain V4051 (van der Drift et al., 1975), a peritrichously flagellated, primarily fermentative, gram-positive organism that lacks an endogenous energy reserve and is sensitive to ionophores and uncouplers. Unlike *E. coli*, this organism can be starved and artificially energized, either with a potassium diffusion potential (by treating cells with valinomycin and shifting them to a medium with a lower concentration of potassium ion) or with a pH gradient (by shifting cells to a medium of lower pH). If this is done with a medium of low buffering capacity, one can follow proton uptake by the increase in external pH. The frequency of rotation of filaments in flagellar bundles can be determined by using power spectral analysis to measure cell vibration frequencies (Lowe et al., 1987). Finally, the data can be normalized to single motors by counting the number of cells and the number of flagellar filaments per cell. The total proton flux into the cell is much larger than the flux through its flagellar motors. However, the two can be distinguished by suddenly stopping the motors by adding an antifilament antibody—this cross-links adjacent filaments in the flagellar bundles—and measuring the change in flux. This change was found to be directly proportional to the initial swimming speed, as would be expected if a fixed number of protons carries a motor through each revolution. This number is about 1200 (Meister et al., 1987) but subject to uncertainty, due mainly to the difficulty of counting flagellar filaments.

Some bacteria, notably marine bacteria or bacteria that live at high pH, use sodium ions instead of protons (Imae, 1991; Imae and Atsumi, 1989). Thus, flagellar motors are ion driven, not just proton driven. For reviews on sodium-driven motors, see McCarter (2001) and Yorimitsu and Homma (2001).

Torque-Generating Units

The flux through the flagellar motor is divided into as many as eight distinct proton channels (or pairs of proton channels), comprising one or more copies of the proteins MotA and MotB (currently thought to be four MotA and two MotB). Evidence for this was obtained by restoring the motility of paralyzed cells (*mot* mutants) via the expression of wild-type genes carried by plasmids. As new protein is synthesized, the speed of tethered cells increases in a number of equally spaced steps, as shown in Fig. 12.1. This indicates that each additional torque-generating unit (comprising MotA and MotB) adds the same increment of torque (applies a similar force at the same distance from the axis of rotation). The main argument for a complement of eight such torque-generating units is that resurrections of this kind have produced eight equally spaced levels more than once, but never nine.

Stepping

It is likely that the passage of each proton (or each proton pair) moves a torque generator (a MotA, MotB complex) one step (one binding site) along the periphery of the rotor, suddenly stretching the components that link that generator to the rigid framework of the cell wall. As this linkage relaxes, a tethered cell should rotate by a fixed increment, once the tether relaxes (see below). In other words, the motor should behave like a stepping motor. Since proton passage is likely to occur at random times, the steps will occur with exponentially distributed waiting times. We have been looking for such steps since 1976 (Berg, 1976) but without success. The main reason, advanced then, is that the torque applied to the structure linking the rotor to the tethering surface (a series of elastic elements, comprising the rod, hook, and filament) causes that structure to twist. When less torque is applied, these elements tend to untwist, carrying the cell body forward. Therefore, discontinuities in the relative motion of rotor and stator are smoothed out. To succeed, one probably needs to work at reduced

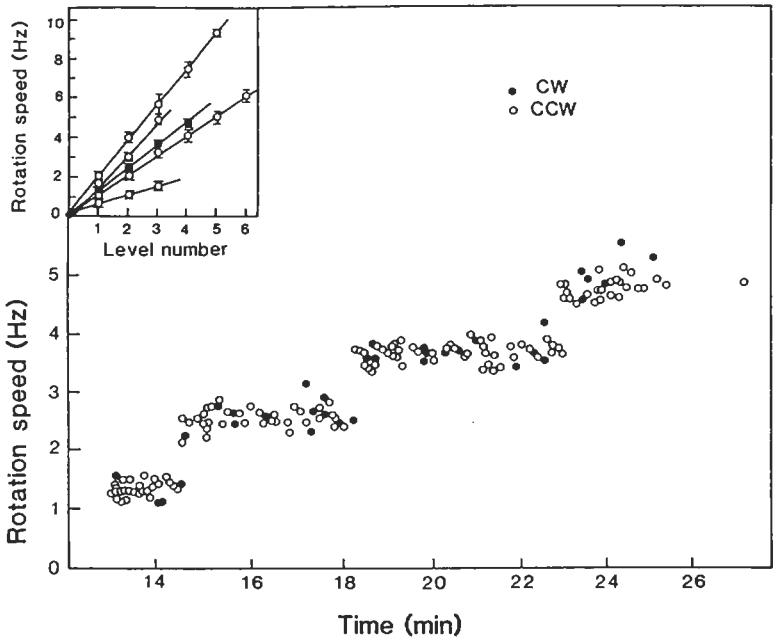

FIGURE 12.1. Rotation speed of a tethered *motA* cell, *E. coli* strain MS5037(pDFB36), following addition (at time 0) of the inducer isopropyl β-D-thiogalactoside (IPTG, added in a minimal medium containing glycerol, glucose, and essential amino acids). Filled circles indicate CW rotation, open circles CCW rotation. The inset shows the mean rotation speed (±standard error of the mean) at each level (step of the staircase) as a function of level number, for this cell (closed circles) and for four additional cells (open circles). (Blair & Berg, 1988, Fig. 1, reprinted with permission from the American Association for the Advancement of Science.)

torque, for example, with a one-generator motor driving a small viscous load, perhaps just a hook. Such an object is expected to spin quite rapidly, so the technical problems are formidable.

One route around this difficulty is to examine variations in rotation period. If n steps occur at random each revolution, then the ratio of the standard deviation to the mean should be $n^{-1/2}$ (see the appendix in Samuel and Berg, 1995), so one can determine n. With tethered wild-type cells, the answer turns out to be about 400. This work also showed that tethered cells are not free to execute rotational brownian motion. Thus, the rotor and stator are interconnected most of the time.

This stochastic analysis was repeated with tethered cells undergoing resurrection (as in Fig. 12.1), and the number of steps per revolution was found to increase linearly with level number, increasing by about 50 steps per level (Samuel and Berg, 1996). If torque generators interact with a fixed number of binding sites on the rotor, say 50, then why is the number of steps per revolution not just 50? If m torque generators are attached to the rotor and one steps, suddenly stretching its linkage to the rigid framework of the cell wall, then when that linkage relaxes and moves the rotor, it also must stretch the linkages of the $m - 1$ torque generators that have not stepped. If $m = 2$, the net movement of the rotor is half of what it would be at $m = 1$, so the apparent step number is 100 per revolution. If $m = 8$, the apparent step number is 400 per revolution. If, on the other hand, each torque generator is detached most of the time (for most of its duty cycle), then the apparent step number would remain 50. So this experiment argues not only that each force generator steps independently of all the others, but that each remains connected to the rotor most of the time. In fact, the torque generators must be attached nearly all of the time (see below).

Torque-Speed Dependence

A crucial test of any motor model is its torque-speed dependence. Measurements of the torque generated by motors of *E. coli* have been made over a wide range of speeds, including speeds in which the motor is driven backward, with the results shown in Fig. 12.2 (thick lines). At 23°C, the torque exerted by the motor is approximately constant, all the way from negative speeds of at least −100 Hz to positive speeds of nearly 200 Hz. At higher speeds it declines approximately linearly, crossing the 0-torque line at about 300 Hz. At lower temperatures, the region of transition from constant torque to declining torque—we call this the "knee"—shifts to lower speeds, and the region of decline steepens (Berg and Turner, 1993; Chen and Berg, 2000a); the latter parts of the curves can be mapped onto one another with scaling of the speed axis.

Estimates of the torque generated in the low-speed regime range from about 2.7×10^{-11} dyn cm (2700 pN nm) to 4.6×10^{-11} dyn cm (4600 pN nm), the smaller value from estimates of the viscous

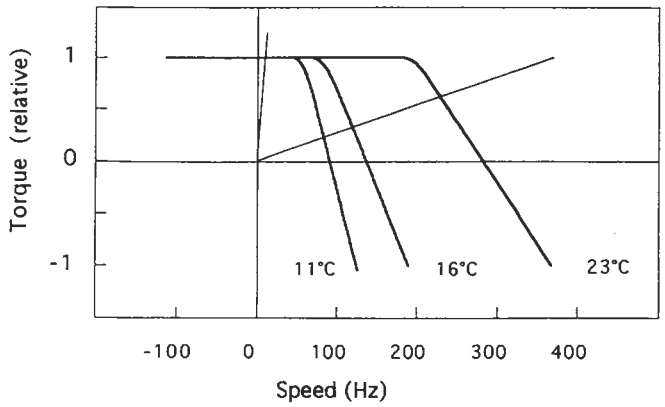

FIGURE 12.2. The torque-speed curve for the flagellar motor of *E. coli* shown at three temperatures (thick lines), together with two load lines (thin lines), one for an object the size of the cell body of wild-type *E. coli* (effective radius about 1 μm, left), the other for a latex bead of radius about 0. 3 μm, right. (Adapted from Fig. 16 of Berg and Turner, 1993.) Later work showed that the torque declines somewhat in the low-speed regime, by about 10% between stall and the knee; see the text.

drag on tethered cells of *Streptococcus* (Lowe et al., 1987), and the larger value from the force exerted by tethered cells of *E. coli* on latex beads held in an optical trap (Berry and Berg, 1997).

A motor driving an inert object (a cell body, a latex bead, etc.) will spin at the speed at which the torque generated by the motor is balanced by the torque exerted on the object by viscous drag. This torque is defined by load lines, such as those shown in Fig. 12.2 (thin lines), the one at the left for a large object and the one at the right for a small object. To see this, note that the torque, N, required to rotate an object of fixed shape in a viscous medium is its rotational frictional drag coefficient, f, times its angular velocity, Ω (2π times its rotation speed, in Hz). In a torque versus speed plot, this function is a straight line passing through the origin, with slope f. Here, we assume that the medium is Newtonian, that is, that the frictional drag coefficient does not depend on Ω, a condition satisfied in a dilute aqueous medium that does not contain long unbranched molecules, such as methylcellulose or polyvinylpyrrolidone (Berg and Turner, 1979). For such a medium, f is a geometrical factor times the bulk viscosity, η, where η is independent of Ω (independent of the rate of shear). For an isolated

sphere of radius a spinning about an axis through its center, for example, this geometrical factor is $8\pi a^3$. For compact globular objects, the actual shape is not very critical; however, accurate values can be computed (Garcia de la Torre and Bloomfield, 1981). The distance from the tethering surface does not really matter, either, provided that the gap between the object and the surface is at least 0.2 cell radii (Berg, 1976; Jeffery, 1915).

At 23°C and for the load line shown at the left in Fig. 12.2, the motor runs at 10 Hz; for the load line shown at the right, it runs about 220 Hz. For a very shallow load line (e.g., one for a free hook), the speed would be close to the zero-torque speed, about 290 Hz. A motor free-running in this way always operates in the upper-right-hand quadrant of Fig. 12.2. It cannot drive itself backward, although it can redefine what is meant by forward by switching from counterclockwise (CCW) to clockwise (CW) or back again. Nor can it spin faster than its speed at zero load. To probe the upper-left-hand or lower-right-hand quadrants of Fig. 12.2, one needs to subject the motor to torque applied externally.

One way to do this is by electrorotation (Washizu et al., 1993). Cells were tethered and exposed to a high frequency (2.25 MHz) rotating electric field (Berg and Turner, 1993). As explained in the latter reference, the external electric field polarizes the cell. The dipole field due to the polarization rotates at the same rate and in the same direction as the applied electric field. However, due to the finite time required for redistribution of charges, the polarization vector leads or lags the electric-field vector. The externally applied torque is the cross-product of these vectors. The applied torque varies as the square of the magnitude of the electric field and changes sign with changes in the direction of rotation of that field. Therefore, it is possible to spin a tethered cell either forward or backward. Speeds of several hundred Hz are readily attainable. For reasons that we do not understand, the motor of a cell driven backward (CW if it is trying to spin CCW, or CCW if it is trying to spin CW) often breaks catastrophically: motor torque suddenly drops to zero, the cell appears free to execute rotational brownian motion, and the motor fails to recover. Our best guess is that the C-ring is sheared off of the bottom of the rotor (Fig. 9.3), disengaging all torque-generating units but leaving the bearings intact. Once the motor has broken, one can compare the speed at which the cell body turns at a given value of externally applied torque with the speed at which it turned at the same value of externally applied torque before the break occurred. That differ-

ence is proportional to the torque generated by the motor at the speed at which it turned when intact. The data shown by the thick lines in Fig. 12.2 were determined in this way.

Additional work on the behavior of the motor in the upper-right-hand quadrant of Fig. 12.2 was done by manipulating load lines. Flagella were shortened by viscous shear, and cells were adsorbed onto positively charged glass. Latex beads of various sizes were attached to the flagellar stubs, and the slopes of their load lines were increased by addition of the viscous agent Ficoll (Chen and Berg, 2000a). In the low-speed regime, torque was found to drop by about 10% from stall to the knee. In this regime, torque was independent of temperature, and solvent isotope effects were relatively small, as found earlier for artificially energized cells of *Streptococcus* (Khan and Berg, 1983). Evidently, at low speeds, the motor operates near thermodynamic equilibrium, where rates of displacement of internal mechanical components or translocation of protons are not limiting. In the high-speed regime, torque was strongly temperature dependent, as seen in Fig. 12.2, and solvent isotope effects were large (Chen and Berg, 2000b). This is what one would expect if the decline in torque at high speed is due to limits in rates of proton transfer (proton dissociation).

Slowly declining torque in the low-speed regime argues for a model in which the rate-limiting step depends strongly on torque and dissipates most of the available free energy, that is, for a powerstroke mechanism, while the absence of a barrier to backward rotation rules out models (e.g., thermal ratchets) that contain a step that is effectively irreversible and insensitive to external torque (Berry and Berg, 1999). Eventually, we would like to understand why the low-speed regime is so broad, why the boundary between the low-speed and high-speed regimes is so narrow, and why the position of that boundary is so sensitive to temperature.

The power output, the power dissipated when a torque N sustains rotation at angular velocity Ω, is $N\Omega$. For torque 4600 pN nm and speed 10 Hz, this is 2.9×10^5 pN nm s^{-1}. The power input, the rate at which protons can do work, is proton flux times proton charge times protonmotive force. Assuming 1200 protons per revolution and speed 10 Hz, the proton flux is 1.2×10^4 s^{-1}. For *E. coli* at pH 7, $\Delta p \approx -170$ mV. Therefore, the power input is $(1.2 \times 10^4 \text{s}^{-1})$ (e) $(0.17\,\text{V}) = 2.0 \times 10^3$ eV s^{-1}. Since 1 eV (one electron volt) $= 1.6 \times 10^{-12}$ erg $= 160$ pN nm, the power input is 3.2×10^5 pN nm s^{-1}. So, by this crude estimate, the efficiency of the motor, power output divided by power input, is about 90%. Within the uncertainty of the measurements—the proton flux has not been measured in *E. coli*—the efficiency could be 1.

The power output, $N\Omega$, increases linearly with speed up to the boundary between the low-speed and high-speed regimes, and then it declines. If a fixed number of protons carries the motor through each revolution, the power input also increases linearly with speed. Therefore, the efficiency remains approximately constant up to the knee, and then it declines. There is no discontinuity in torque as one crosses the zero-speed axis (Berry and Berg, 1997). As the motor turns backward, it must pump protons, just as the F_0-ATPase pumps protons when driven backward by F_1.

The force exerted by each force-generating unit is substantial but not large on an absolute scale. If we take a ballpark figure for the stall torque of 4000 pN nm and assume that force-generating units act at the periphery of the rotor at a radius of about 20 nm, then 200 pN is applied. If there are eight independent force-generating units, then each contributes 25 pN. This is a force equal in magnitude to that between two electrons 4.8 angstroms apart in a medium of dielectric constant 40 (midway between water, 80, and lipid, about 2). So almost any kind of chemistry will do.

The energy available from one proton moving down the electrochemical gradient is $e\Delta p$. Given $\Delta p \approx -170$ mV, this is 0.17 eV, or 27 pN nm. At unit efficiency, this equals the work that the force-generator can do, Fd, where F is the force that it exerts, and d is the displacement generated by the transit of one proton. Assuming 52 steps per revolution (twice the number of FliG subunits) and a rotor radius of 20 nm, d $\approx$ 2.4 nm. So $F \approx 11$ pN. If two protons are required per elementary step, the force is twice as large, and $F \approx 22$ pN. So, given the estimate of 25 pN per force-generating unit made above, the displacement of two protons per step is likely.

Angular Dependence of Torque

When optical tweezers were used to drive cells slowly backward or to allow them to turn slowly forward (Berry & Berg, 1997), torque did not vary appreciably with angle. A very different result

is obtained when one energizes and de-energizes tethered cells and asks where they stop or watches them spin when the proton-motive force is very low. When this was done with *Streptococcus*, periodicities were observed of order 5 or 6 (Khan et al., 1985). This probably reflects small periodic barriers to rotation intrinsic to the bearings.

Duty Ratio

In our stochastic analysis of steps (above) we argued that the apparent number of steps per revolution would increase with the number of torque generators, as observed, if each torque generator remained attached to the rotor most of the time, that is, if the torque-generating units had a high duty ratio. The following argument shows that the duty ratio must be close to 1. Evidently, torque generators, like molecules of kinesin, are processive. Consider a tethered cell being driven by a single torque-generating unit, as in the first step of the resurrection shown in Fig. 12.1. If a wild-type motor with eight torque-generating units generates a torque of about 4×10^{-11} dyn cm (4000 pN nm), then the single-unit motor generates a torque of about 5×10^{-12} dyn cm. The torsional spring constant of the tether—most of the compliance is in the hook—is about 5×10^{-12} dyn cm rad^{-1} (Block et al., 1989), so the tether is twisted up about 1 radian, or 57 degrees. Now the viscous drag on the cell body is enormous compared to that on the rotor, so if the torque-generating unit lets go, the tether will unwind, driving the rotor backward. If the single unit steps 50 times per revolution, the displacement is 7.2 degrees per step. If the cell is spinning ~1.2 Hz (Fig. 12.1), the step interval is 1.6×10^{-2} s. If the duty ratio is 0.999, so that the torque-generating unit detaches for 1.6×10^{-5} s during each cycle, how far will the tether unwind? The tether unwinds exponentially: $\theta = \theta_0 \exp(-\alpha t)$, where θ_0 is the initial twist, and α is the torsional spring constant divided by the rotational frictional drag coefficient. If we approximate the rotor as a sphere of radius $a = 20$ nm immersed in a medium of viscosity $\eta = 1$ P (1 g cm^{-1} s^{-1}), which is about right for a lipid membrane, then the frictional drag coefficient, $8\pi\eta a^3$, is 2×10^{-16} dyn cm per rad s^{-1}, and $\alpha = 2.5 \times 10^4$ s^{-1}. So, in 1.6×10^{-5} s, the twist in the tether decreases from 57 degrees to 57 $\exp(-2.5 \times 10^4 \text{ s}^{-1} \times 1.6 \times 10^{-5} \text{ s}) =$ 38 degrees, or by 19 degrees, that is, by more than twice the step angle. Thus, the torque-generating unit would not be able to keep up. So the duty ratio must be close to 1. The interaction between the torque-generating unit and the rotor must be such that the rotor is not able to slip backward. If one imagines that a torque-generating unit binds to successive sites along the periphery of the rotor, then it has no unbound states. If each torque-generating unit has two proton channels (Braun and Blair, 2001), it is possible that a MotA associated with one channel remains attached to a FliG, while the MotA associated with the other channel takes the next step.

Switching

Finally, the motor can run in either direction with approximately equal efficiency. Although the force-generating elements move independently, they all switch at the same time: changes in direction occur in an all-or-none fashion within a few milliseconds. Evidently, the rotor suddenly changes shape, so that the force-generating elements step along a different track. What sort of change in conformation occurs? And why is this process so sensitive to the concentration of CheY-P?

Models

The fundamental question is how the flagellar motor generates torque, namely, how inward motion of one or more ions through a torque-generating unit causes it to advance circumferentially along the periphery of the rotor. Once that is understood, the nature of the conformational change required for switching, namely, how the direction of advance is distinguished from that of retreat, is likely to be self-evident.

Moving parts of the motor are submicroscopic and immersed in a viscous medium (water or lipid), so the Reynolds number is very small (see Chapter 6). And everything is overdamped (Howard, 2001, pp. 41–45). Thus, the designer does not have the benefit of flywheels or tuning forks. If, for example, the operator of the motor driving a tethered cell of *E. coli* 10 Hz were to put in the clutch, the cell body would coast no more than a millionth of a revolution. So if there is a stage in the rotational cycle in which the torque changes sign, the motor will stop. Predicting net torque after averaging over a complete cycle is not sufficient. And mech-

anisms in which energy is stored in vibrational modes are not viable. However, one can use energy available from an electrochemical potential to stretch a spring and then use that spring to apply a steady force. As we have seen, the force required is modest, and almost any kind of chemistry will do.

Motion of the torque-generating units relative to the periphery of the rotor is driven by a proton (or sodium-ion) flux. Only one experiment has attempted to measure this flux (Meister et al., 1987), and flux and speed were found to be linearly related. Unless protons flow through the motor when it is stalled, this implies that a fixed number of protons carry the motor through each revolution. The running torque at low speeds is close to the stall torque (Fig. 12.2). If the motor is stalled and no protons flow, no free energy is dissipated; therefore, the stalled motor is at thermodynamic equilibrium. For slow rotation near stall, the motor must operate reversibly at unit efficiency, with the free energy lost by protons traversing the motor equal to the mechanical work that it performs. This implies that the torque near stall should be proportional to the protonmotive force over its full physiological range, as observed. So the evidence is consistent with a model in which the motor is tightly coupled.

An important question is whether the ion that moves down the electrochemical gradient is directly involved in generating torque, that is, participates in a powerstroke in which dissipation of energy available from the electrochemical gradient and rotational work occur synchronously, or whether the ion is indirectly involved in generating torque (e.g., by enabling a ratchet that is powered thermally). In the powerstroke case, protons can be driven out of the cell by backward rotation, and steep barriers are not expected. In addition, if the rate-limiting step is strongly torque dependent, then the torque-speed curve (as plotted in Fig. 12.2) can have a relatively flat plateau, because small changes in torque can generate large changes in speed. In the ratchet case, with tight coupling, the likelihood of transit of ions against the electrochemical gradient is small, so the system must wait, even when large backward torques are applied, and barriers to backward rotation are expected. So the torque-speed curves of Fig. 12.2 favor a powerstroke mechanism.

There appear to be essential electrostatic interactions between specific residues in the cytoplasmic domain of MotA and the C-terminal domain of FliG (Zhou et al., 1998a). Here, charge

complementarity is more important than surface complementarity; that is, long-range interactions appear to be more important than tight binding. Since some models for torque generation require transfer of protons from the stator to the rotor, it was expected that acidic residues on FliG might be more important than basic residues. However, replacement of the acidic residues deemed important for torque generation with alanine still allowed some rotation, while reversing their charge had a more severe effect (Lloyd and Blair, 1997). An extension of this study failed to identify any conserved basic residues critical for rotation in MotA, MotB, FliG, FliM, or FliN, and only one conserved acidic residue critical for rotation, Asp32 of MotB (Zhou et al., 1998b). Other alternatives were considered and either ruled out or deemed unlikely. Therefore, the only strong candidate for a residue that functions directly in proton conduction is Asp32 of MotB.

MotA and MotB appear to form a cassette containing a transmembrane channel that supports proton flow, generating transformations that drive movement along the periphery of the rotor. That the ion-dependence is determined solely by MotA and MotB (or their homologs) has been shown conclusively in recent experiments in which transmembrane and cytoplasmic domains of MotA and MotB were replaced by homologous parts of PomA and PomB, from *Vibrio alginolyticus*. With only the C-terminal periplasmic domain of MotB remaining, the *E. coli* motor became sodium-ion driven rather than proton driven (Asai et al., 2003).

Given the above work, I would bet on a cross-bridge mechanism of the kind that Blair and colleagues propose (Braun et al., 1999; Kojima and Blair, 2001). In such a scheme, proton transport drives a cyclic sequence in which (1) a proton binds to an outward-facing binding site; (2) the protonmotive force drives a conformational change, a powerstroke that moves the rotor forward (or stretches a spring that moves it forward) and transforms the binding site to an inward-facing site; and (3) proton dissociation triggers detachment of the cross-bridge from the rotor, its relaxation to the original shape, and reattachment to an adjacent site. If the MotA/MotB complex is two-headed, one head could remain attached while the other stepped, thus ensuring a high duty ratio.

But to be honest, we really do not understand how the motor works, i.e., how proton translocation generates torque. Modeling would help, but what is needed most is more structural information.

Reviews

For other reviews on the structure and function of proton-driven motors, see Läuger and Kleutsch (1990), Caplan and Kara-Ivanov (1993), Schuster and Khan (1994), Macnab (1996), Khan (1997), Berry and Armitage (1999), Berry (2000, 2003), Berg (2000, 2003), and Blair (2003). For a catalog of early models, see Berg and Turner (1993). For tutorials on the mathematical treatment of motor models, see Berry (2000) and Bustamante et al. (2001). The material in this chapter was adapted from Berg (2003).

References

Asai, Y., T. Yakushi, I. Kawagishi, and M. Homma. 2003. Ion-coupling determinants of Na^+-driven and H^+-driven flagellar motors. *J. Mol. Biol.* 327:453–463.

Berg, H. C. 1976. Does the flagellar rotary motor step? In: Cell Motility, Cold Spring Harbor Conferences on Cell Proliferation. R. Goldman, T. Pollard, J. Rosenbaum, editors. Cold Spring Harbor Laboratory, Cold Spring Harbor, NY, pp. 47–56.

Berg, H. C. 2000. Constraints on models for the flagellar rotary motor. *Philos. Trans. R. Soc. Lond. B* 355:491–501.

Berg, H. C. 2003. The rotary motor of bacterial flagella. *Annu. Rev. Biochem.* 72:19–54.

Berg, H. C., and L. Turner. 1979. Movement of microorganisms in viscous environments. *Nature* 278:349–351.

Berg, H. C., and L. Turner. 1993. Torque generated by the flagellar motor of *Escherichia coli*. *Biophys. J.* 65:2201–2216.

Berry, R. B. 2000. Theories of rotary motors. *Philos. Trans. R. Soc. Lond. B* 355:503–509.

Berry, R. B. 2003. The bacterial flagellar motor. In: Molecular Motors. M. Schliwa, editor. Wiley-VCH, Weinheim, pp. 111–140.

Berry, R. B., and J. P. Armitage. 1999. The bacterial flagella motor. *Adv. Microbiol. Physiol.* 41:291–337.

Berry, R. M., and H. C. Berg. 1997. Absence of a barrier to backwards rotation of the bacterial flagellar motor demonstrated with optical tweezers. *Proc. Natl. Acad. Sci. USA* 94:14433–14437.

Berry, R. M., and H. C. Berg. 1999. Torque generated by the flagellar motor of *Escherichia coli* while driven backward. *Biophys. J.* 76: 580–587.

Blair, D. F. 2003. Flagellar movement driven by proton translocation. *FEBS Lett.* 545:86–95.

Blair, D. F., and H. C. Berg. 1988. Restoration of torque in defective flagellar motors. *Science* 242:1678–1681.

Block, S. M., D. F. Blair, and H. C. Berg. 1989. Compliance of bacterial flagella measured with optical tweezers. *Nature* 338:514–517.

Braun, T. F., and Blair, D. F. 2001. Targeted disulfide cross-linking of the MotB protein of *Escherichia coli*: evidence for two H^+ channels in the stator complex. *Biochemistry* 40:13051–13059.

Braun, T. F., S. Poulson, J. B. Gully, et al. 1999. Function of proline residues of MotA in torque generation by the flagellar motor of *Escherichia coli*. *J. Bacteriol.* 181:3542–3551.

Bustamante, C., D. Keller, and G. Oster. 2001. The physics of molecular motors. *Acc. Chem. Res.* 34:412–420.

Caplan, S. R., and M. Kara-Ivanov. 1993. The bacterial flagellar motor. *Int. Rev. Cytol.* 147:97–164.

Chen, X., and H. C. Berg. 2000a. Torque-speed relationship of the flagellar rotary motor of *Escherichia coli*. *Biophys. J.* 78:1036–1041.

Chen, X., and H. C. Berg. 2000b. Solvent-isotope and pH effects on flagellar rotation in *Escherichia coli*. *Biophys. J.* 78:2280–2284.

Fung, D. C., and H. C. Berg. 1995. Powering the flagellar motor of *Escherichia coli* with an external voltage source. *Nature* 375:809–812.

Gabel, C. V., and H. C. Berg. 2003. The speed of the flagellar rotary motor of *Escherichia coli* varies linearly with protonmotive force. *Proc. Natl. Acad. Sci. USA* 100:8748–8751.

Garcia de la Torre, J., and V. A. Bloomfield. 1981. Hydrodynamic properties of complex, rigid, biological macromolecules: theory and applications. *Q. Rev. Biophys.* 14:81–139.

Harold, F. M., and P. C. Maloney. 1996. Energy transduction by ion currents. In: *Escherichia coli* and *Salmonella*: Cellular and Molecular Biology. F. C. Neidhardt, R. Curtiss, J. L. Ingraham, et al., editors. ASM Press, Washington DC, pp. 283–306.

Howard, J. 2001. Mechanics of Motor Proteins and the Cytoskeleton. Sinaur Associates, Sunderland, MA.

Imae, Y. 1991. Use of Na^+ as an alternative to H^+ in energy transduction. In: New Era of Bioenergetics. Y. Mukohata, editor. Academic Press, Tokyo, pp. 197–221.

Imae, Y., and T. Atsumi. 1989. Na^+-driven bacterial flagellar motors. *J. Bioenerg. Biomembr.* 21:705–716.

Jeffery, G. B. 1915. On the steady rotation of a solid of revolution in a viscous fluid. *Proc. Lond. Math. Soc.* 14:327–338.

Khan, S. 1997. Rotary chemiosmotic machines. *Biochim. Biophys. Acta* 1322:86–105.

Khan, S., and H. C. Berg. 1983. Isotope and thermal effects in chemiosmotic coupling to the flagellar motor of *Streptococcus*. *Cell* 32:913–919.

Khan, S., M. Meister, and H. C. Berg. 1985. Constraints on flagellar rotation. *J. Mol. Biol.* 184:645–656.

Kojima, S., and D. F. Blair 2001. Conformational change in the stator of the bacterial flagellar motor. *Biochemistry* 40:13041–13050.

Larsen, S. H., J. Adler, J. J. Gargus, and R. W. Hogg. 1974. Chemomechanical coupling without ATP: the source of energy for motility and chemotaxis in bacteria. *Proc. Natl. Acad. Sci. USA* 71:1239–1243.

Läuger, P., and B. Kleutsch. 1990. Microscopic models of the bacterial flagellar motor. *Comments Theor. Biol.* 2:99–123.

Lloyd, S. A., and D. F. Blair. 1997. Charged residues of the rotor protein FliG essential for torque generation in the flagellar motor of *Escherichia coli*. *J. Mol. Biol.* 266:733–744.

Lowe, G., M. Meister, and H. C. Berg. 1987. Rapid rotation of flagellar bundles in swimming bacteria. *Nature* 325:637–640.

Macnab, R. M. 1996. Flagella and motility. In: *Escherichia coli* and *Salmonella*: Cellular and Molecular Biology. F. C. Neidhardt, R. Curtiss, J. L. Ingraham, et al., editors. ASM Press, Washington, DC, pp. 123–145.

McCarter, L. L. 2001. Polar flagellar motility of the *Vibrionaceae*. *Microbiol. Mol. Biol. Rev.* 65:445–462.

Meister, M., G. Lowe, and H. C. Berg. 1987. The proton flux through the bacterial flagellar motor. *Cell* 49:643–650.

Ravid, S., and M. Eisenbach. 1984. Minimal requirements for rotation of bacterial flagella. *J. Bacteriol.* 158:1208–1210.

Samuel, A. D. T., and H. C. Berg. 1995. Fluctuation analysis of rotational speeds of the bacterial flagellar motor. *Proc. Natl. Acad. Sci. USA* 92: 3502–3506.

Samuel, A. D. T., and H. C. Berg. 1996. Torque-generating units of the bacterial flagellar motor step independently. *Biophys. J.* 71:918–923.

Schuster, S. C., and S. Khan. 1994. The bacterial flagellar motor. *Annu. Rev. Biophys. Biomol. Struct.* 23:509–539.

van der Drift, C., J. Duiverman, H. Bexkens, and A. Krijnen. 1975. Chemotaxis of a motile *Streptococcus* toward sugars and amino acids. *J. Bacteriol.* 124:1142–1147.

Washizu, M., Y. Kurahashi, H. Iochi, et al. 1993. Dielectrophoretic measurement of bacterial motor characteristics. *IEEE Trans. Ind. Appl.* 29:286–294.

Yorimitsu, T., and M. Homma. 2001. Na^+-driven flagellar motor of *Vibrio*. *Biochim. Biophys. Acta* 1505:82–93.

Zhou, J., S. A. Lloyd, and D. F. Blair. 1998a. Electrostatic interactions between rotor and stator in the bacterial flagellar motor. *Proc. Natl. Acad. Sci. USA* 95:6436–6441.

Zhou, J., L. L. Sharp, H. L. Tang, et al. 1998b. Function of protonatable residues in the flagellar motor of *Escherichia coli*: a critical role for Asp 32 of MotB. *J. Bacteriol.* 180:2729–2735.

13
Epilogue

What We Have Learned

I have told you some things about a free-living organism only one micron in size. It is equipped with sensors that count molecules of interest in its environment, coupled to a readout device that computes whether these counts are going up or down. The output is an intracellular signal that modulates the direction of rotation of a set of rotary engines, each turning a propeller with variable pitch. Each engine (or motor) is driven, in turn, by several force-generating elements (like pistons), powered by a transmembrane ion flux. In addition to a gear shift (labeled forward and reverse but prone to shift on its own) there is a stator, a rotor, a drive shaft, a bushing, and a universal joint.

We know a great deal about what all this machinery does for the bacterium, a fair amount about the structures of the molecular components involved (particularly those that have been crystallized), and even how the organism programs their syntheses. We know less about the precise ways in which these components function.

Levels of Amazement

Some wonder how the flagellar motor possibly could have evolved. The problem here is that we do not know about earlier states. What was the flagellar motor doing, for example, before the acquisition of the propeller (if, indeed, that was the sequence of events)? Perhaps it was winding up DNA. Or maybe it was injecting toxins into other cells as part of a program of conquest. In any event, it must have been doing something that promoted the survival of the organism. Evolution is opportunistic: it builds on components already at hand. One can not turn off the organism